Contents lists available at GrowingScience

Current Chemistry Letters

homepage: www.GrowingScience.com

Influence of temperature on the magnetic properties of Mn_3O_4 nanowires

Sangaraju Sambasivam[a], Yedluri Anil Kumar[b], Chandu V.V. Muralee Gopi[c], Venkatesha Narayanaswamy[d] and Ihab M. Obaidat[a*]

[a]*Department of Physics, United Arab Emirates University, Al Ain -15551, UAE*
[b]*School of Electrical Engineering, Pusan National University, Busan, 46241, South Korea*
[c]*Department of Electrical Engineering, University of Sharjah, Sharjah, P.O. Box 27272, UAE*
[d]*Department of Geology, United Arab Emirates University, Al-Ain 15551, UAE*

C H R O N I C L E

Article history:
Received October 1, 2020
Received in revised form
November 30, 2020
Accepted January 12, 2021
Available online
January 12, 2021

Keywords:
Mn_3O_4 single crystal
Nanowires
TEM
ESR
Ferrimagnetism

A B S T R A C T

Single crystalline Mn_3O_4 nanowires have been synthesized with tetragonal hausmannite structure using a solvothermal method. The structural and morphological evolution of Mn_3O_4 nanowires have been characterized using powder X-ray diffraction, transmission electron microscopy, and electron resonance spectroscopy. The nanowires were grown uniformly along the (200) direction with a diameter of 5–10 nm range. A relatively broad and intense electron spin resonance (ESR) signal was observed at room temperature, with the g ≅ 2.0. As the synthesis temperature increases from 150 to 250 °C, a decrease in ESR signal intensity and line widths were observed. Mn_3O_4 displayed a positive Curie-Weiss temperature, θ, which decreases with the increase of synthesis temperature.

1. Introduction

One of the recent developments in the field of nanomaterials is the ability to tune the physical/chemical properties as a function of synthesis temperature, morphology, and homogeneity of the samples. This process enables us to extract the properties reversibly in a controlled and more systematic manner.[1] In addition, magnetic properties of nanoparticles can be altered by several factors such as particle size, inter-particle interactions,[2] core-shell exchange interactions,[3] and surface effects.[4] Manganese-based oxides have been used extensively in the field of rechargeable batteries, catalysis, gas sensors, solar cells, photo-electrochemical, and magnetic resonance imaging due to their low costs, elemental availability (5th Most abundant metal in the earth's crust) and environmental friendliness.[5] The manganese oxides, MnO, and Mn_3O_4 can attain different crystalline structures depending on the synthesis condition. In the case of Mn_3O_4, two polymorphs are possible: the stable tetragonal (α-Mn_3O_4) and cubic (γ- Mn_3O_4) phases. The most stable α- Mn_3O_4 phase at room temperature has a tetragonal spinel structure containing both di- and trivalent manganese which is represented as

* Corresponding author. Tel.: +971 03-7136321
E-mail address: iobaidat@uaeu.ac.ae (I. M. Obaidat)

doi: 10.5267/j.ccl.2021.1.004

$Mn^{2+}(Mn^{3+})_2O_4$. Where the Mn^{3+} ions are located at the octahedral crystallographic sites and Mn^{2+} ions are located at the tetrahedral crystallographic sites within the spinel structure.[6]

The large-scale synthesis of nanocrystalline manganese oxides with well-defined morphology, composition homogeneity, and oxidation state is a bigger concern.[7-11] For example; Zhang et al. reported a low-temperature solvothermal route and made nanocrystalline Mn_3O_4. However, the method involves an intermediate preparation step of γ-MnOOH nanowires.[12] Yang et al. reported a controlled synthesis of Mn_3O_4 nanocrystals by solvothermal route at 140-160º/24 h. When the reaction time prolonged to 48 h a secondary phase of $MnCO_3$ appeared.[13] For using a solvothermal method, one should focus on reaction temperature and time, which eventually leads to non-agglomerated homogeneous nanoparticles. The present study mainly focuses on the improvement of a solvothermal route for the preparation of homogenous, single crystalline Mn_3O_4 nanowires. In addition, the study involves an understanding of the basic structure, morphology, and magnetic properties under different synthesis conditions as they are of a prime requisite for the large-scale production of phase pure samples with controlled structure. We report the presence of Mn^{3+} by ESR spectroscopy, and the antiferromagnetic behavior of Mn_3O_4 nanowires.

2. Materials and Methods

Mn_3O_4 nanowires were synthesized using a solvothermal technique; all the chemicals used in this synthesis were obtained from Sigma-Aldrich with purity greater than 99%. A stoichiometric amount of alcoholic $MnCl_2$ solution was prepared using ethanol and ethylene glycol as a surfactant in aqueous solution. The pH of the solution mixture was adjusted to 11 using NaOH and transferred into a 60 ml Teflon lined stainless steel autoclave. The sealed autoclave was heated at temperatures 150, 175, 200, and 250 °C for 20 h. The product obtained was separated using a centrifuge and washed with water/ethanol mixture and finally dried at 60 ºC for 24 h. Powder X-ray diffraction pattern (PXRD) of nanopowders was obtained using Phillips X'PERT PRO diffractometer with CuK_α radiation source. The nanowire morphology and phase were obtained using a JEOL 2010 high-resolution transmission electron microscope with an accelerating voltage of 200 kV. ESR spectra of nanowires were obtained at room temperature using X-Band JEOL, JES PX 2300 spectrometer. The magnetic measurements were carried out using SQUID, Quantum Design MPMS-XL7.

3. Results and discussion

The PXRD patterns of Mn_3O_4 nanowires synthesized at different temperatures are shown in **Fig. 1**. All the diffraction peaks were indexed to the tetragonal hausmannite Mn_3O_4 structure (JCPDS card No 24-0734). The diffraction peak becomes sharp and the intensity of the peak increases with increase in annealing temperature from 150 to 250 ºC because of the increase in crystallite size. The crystallite sizes calculated from PXRD data are 28.4 to 43.2 nm for the samples annealed at 150 to 250 ºC. **Fig. 2(a)** shows a typical TEM image of Mn_3O_4 nanowires made at 150 °C/20 h. The diameter and length of the single nanowire Mn_3O_4 is around 5 nm and more than 2 μm, respectively. TEM image of the sample showed that the Mn_3O_4 nanowires are structurally uniform without crystalline defects; such as stacking faults and dislocations. Mn_3O_4 wires have a needle-like morphology without sharp edges, which is expected from the solvothermal method. The concentration of the solution was found to have a significant effect on the formation of the nanowires, high Mn concentration leads to aggregation of nanowires. SAED patterns of the nanowire revealed perfectly crystalline nature with tetragonal structure (**Fig. 2b**) and showed bright lattice fringes with d-spacing 0.273 nm, which is equal to the inter planar distance of the (200) plane of Mn_3O_4 (**Fig. 2c**).

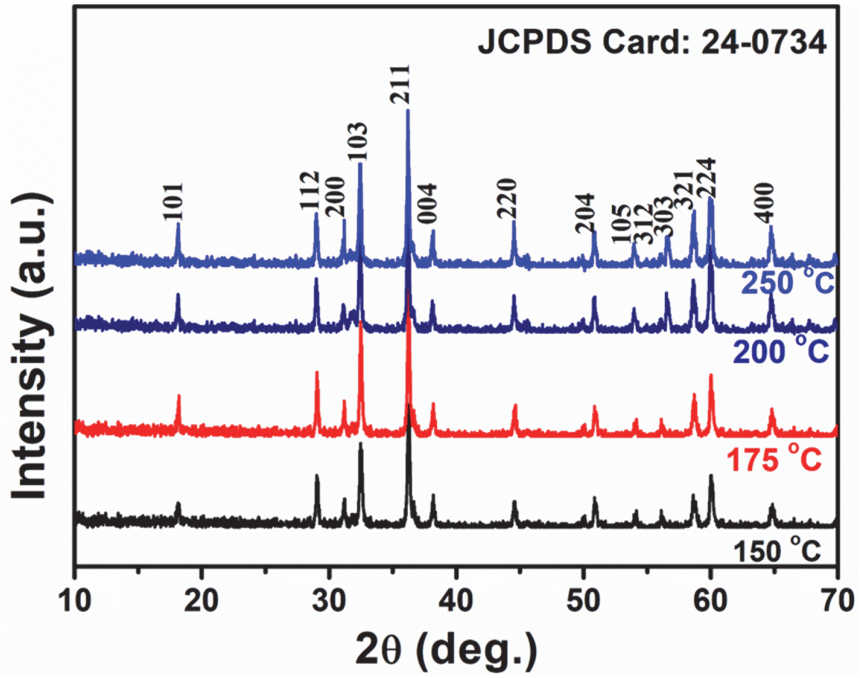

Fig. 1. Powder X-ray diffraction patterns of the Mn_3O_4 nanowires synthesized at various temperatures

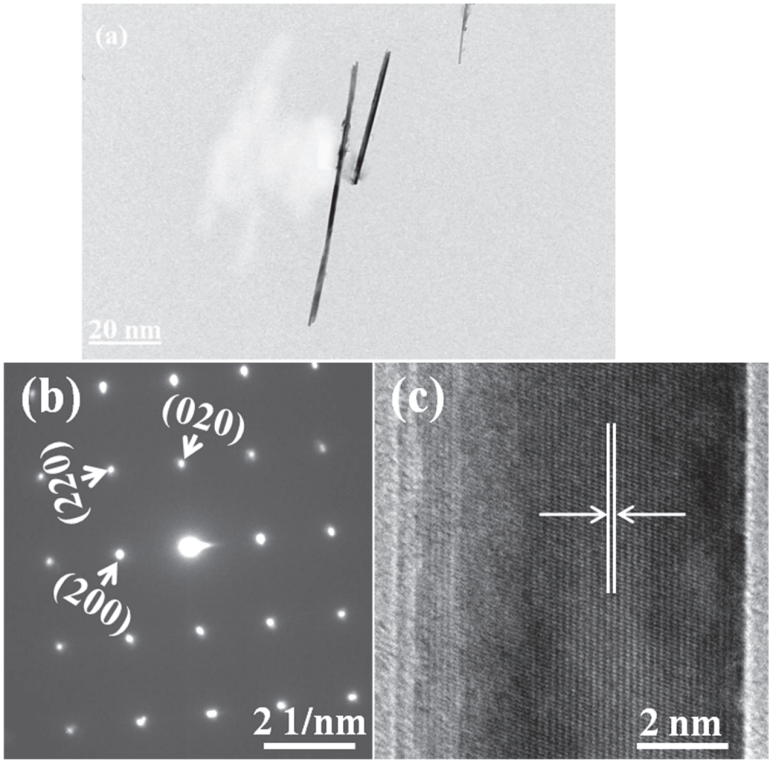

Fig. 2. (a) TEM image (b) SAED pattern, (c) HR-TEM images of Mn_3O_4 nanowires synthesized at 150 ºC/20h.

3.1 ESR and Magnetism

Fig. 3 shows the room-temperature ESR spectra of Mn_3O_4 nanowires annealed at different temperatures between 150 to 250 °C. Intensity of the ESR signal decreases as the temperature increases due to the induced magnetic field (exchange anisotropy field), which is the primary source of magnetic moment for these systems. The ESR spectra composed of a single and relatively broad peak for all samples, whereas the absence of hyperfine splitting suggests that Mn^{3+} cations are well separated. The observed single broad peak is isotropic, suggesting that Mn^{3+} present in octahedral site symmetry. The broadening and shift of the center of resonance to the lower fields are due to the presence of the non-homogenous local magnetic field, which modifies the resonance field and signals shapes. The neutron diffraction studies of Mn_3O_4 show that Mn^{2+} ions are located at the tetrahedral sites, whereas the Mn^{3+} ions are located at the octahedral sites.[14] The calculated Lande 'g' values using $g = h\upsilon/\mu_B H_r$ (where υ, μ, and H_r are microwave frequency, Bohr magnetron, and resonance field respectively) are given in **Table 1**.

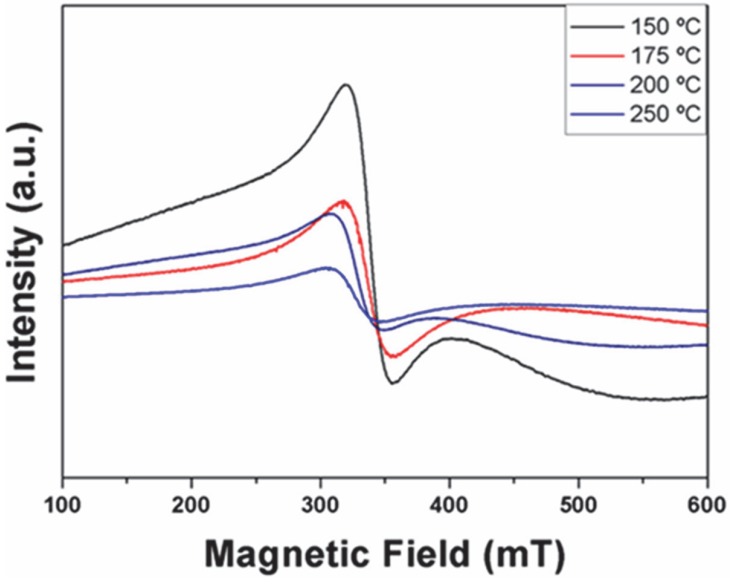

Fig. 3. ESR spectra of Mn_3O_4 nanowires prepared at various temperatures

Table 1. Synthesis temperature, g-values, line width (ΔH) of Mn_3O_4 nanowires are listed

Synthesis temperature (^{0}C)	g-values	ΔH (mT)
150	2.000	36.89
175	2.011	35.9
200	2.052	31.59
250	2.064	29.0

The zero-field-cooled (ZFC) and field-cooled (FC) magnetization versus temperature (M-T) curves are shown in **Fig. 4**. The FC-ZFC and M-T curves show weak bifurcation below 50 K. **Fig. 4(C)** shows a small kink around 10 K, which is attributed to the antiferromagnetic Neel transition temperature T_N and magnetization is attributed to the specific directional (200) growth and morphology of the as synthesized Mn_3O_4 nanowires. The increase in magnetization below 80 K is attributed to the suppression effect of thermal agitation of non-interacting magnetic moments causing the associated paramagnetic contribution.[15] The Curie-Weiss temperature 'θ' estimated from the $1/\chi$ curves (shown in the inset of **Fig. 4**) is found to be 32 K for sample annealed at 150 ºC, 29 K for the sample annealed at 175 ºC, and -14 K for the sample annealed at 250 ºC. The sample synthesized at 150 and 175 ºC have

positive Curie-Weiss temperature indicating positive susceptibility due to the presence of spin canting in the samples. Curie-Weiss temperature shifts to the negative value with synthesis temperature 250 ºC indicating the antiferromagnetic ordering.

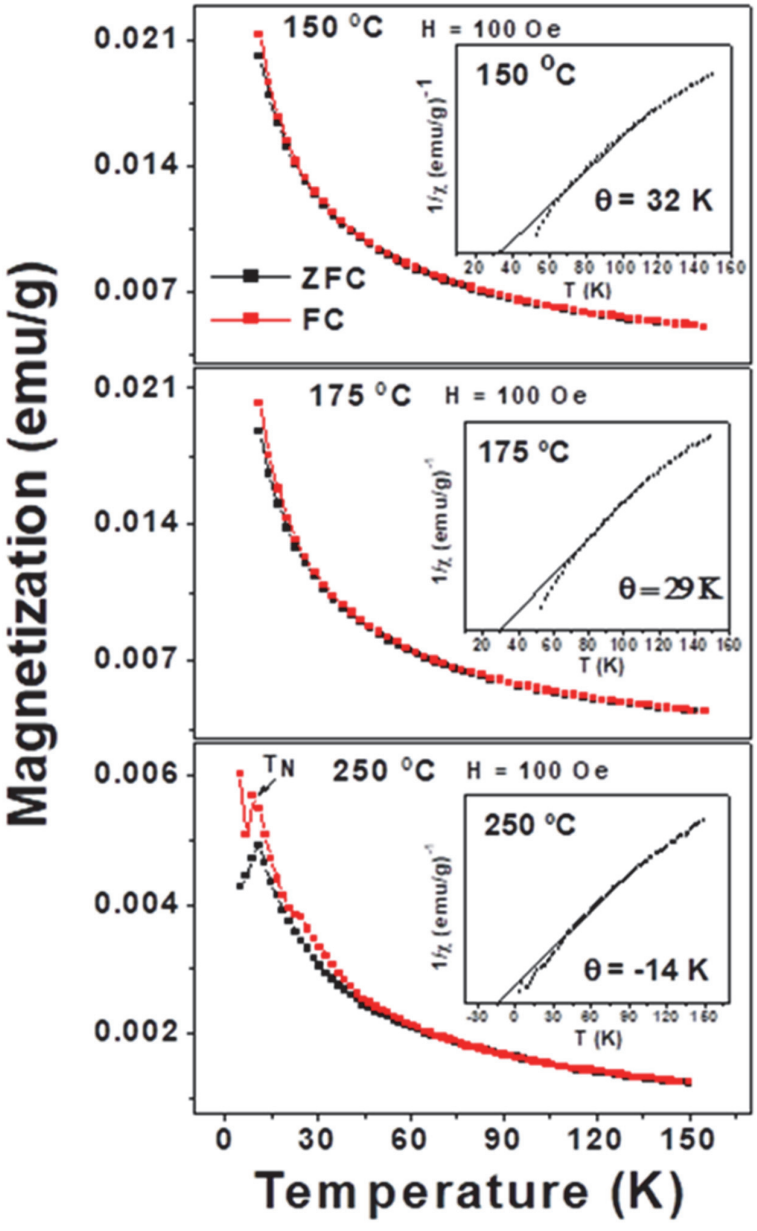

Fig. 4. M-T curves of Mn_3O_4 nanowires samples synthesized at temperatures (a) 150 ºC (b) 175 ºC and (c) 250 ºC. Inset shows the inverse susceptibility *vs.* temperature of the same

4. Conclusions

Single-crystalline Mn_3O_4 nanowires were synthesized by the solvothermal method. The structure, morphological, ESR, and magnetization studies were carried out as a function of synthesis temperature. The powder X-ray diffraction revealed the tetragonal hausmannite structure, whereas ESR spectra confirms that the Mn3+ ions present in the octahedral environment. The intensity of the ESR resonance signal decreases with the increasing synthesis temperature due to the enhanced exchange interaction that arises from the inhomogeneous Mn distribution. Curie-Weiss temperature provided the evidence

for the existence of antiferromagnetic interactions in the sample, which evolved as a function of synthesis temperature. Through the current study, we propose a simple, safe, and low-cost solvothermal method to synthesize large-scale homogenous single crystalline nanowires of manganese oxide. In addition, the magnetic properties can be tuned as a function of synthesis temperature.

Acknowledgment

This work was financially supported by UAEU Program for Advanced Research (UPAR) under Grant no. 31S312.

References

1 Zhai Y., Zhai J., Zhou M., and Dong S. J. **(2009)** Ordered magnetic core–manganese oxide shell nanostructures and their application in water treatment. *J. Mater. Chem.* 19 (38) 7030-7035.

2 Obaidat I. M., Issa B., and Haik Y. **(2011)** The role of aggregation of ferrite nanoparticles on their magnetic properties. *J. Nanosci. Nanotech*. 11 (5) 3882-3888.

3 Obaidat I. M., Nayek C., Manna K., Bhattacharya G., Al-Omari I. A., and Gismelseed A. **(2017)** Investigating exchange bias and coercivity in Fe_3O_4–γ-Fe_2O_3 core–shell nanoparticles of fixed core diameter and variable shell thicknesses. *Nanomater.* 7 (12) 415.

4 Obaidat I. M., Mohite V., Issa B., Tit N., and Haik Y. **(2009)** Predicting a major role of surface spins in the magnetic properties of ferrite nanoparticles. *Cryst. Res. Technol.* 44 (5) 489-494.

5 Baies R., Pralong V., Caignaert V., Saradhi M.P., Varadaraju U.V., and Raveau B. **(2008)** New layered hydrogenophosphate, protonic conductor: $Mn(H_2PO_4)_2$. *Inorg. Chem*. 47 (13) 6072-6076.

6 Sinha A. K., Pradhan M., and Pal T. **(2013)** Morphological evolution of two-dimensional MnO_2 nanosheets and their shape transformation to one-dimensional ultralong MnO_2 nanowires for robust catalytic activity. *J. Phys. Chem. C.* 117 (45) 23976-23986.

7 Luo Y., Yang T., Li Z., Xiao B., and Zhang M. **(2016)** High performance of Mn_3O_4 cubes for supercapacitor applications. *Mater. Lett*. 178 (1) 171-174.

8 Wang L., Chen L., Li Y., Ji H., and Yang G. **(2013)** Preparation of Mn_3O_4 nanoparticles at room condition for supercapacitor application. *Powder Techn*. 235 (1) 76-81.

9 Folkman S. J., Zhou M., Nicki M., and Finke R. G. **(2018)** Alcohol solvent effects in the synthesis of Co_3O_4 metal-oxide nanoparticles: Disproof of a surface-ligand thermodynamic effect an route to alternative kinetic and thermodynamic explanations. *Inorg. Chem*. 57 (3) 1517-1526.

10 Omomo Y., Sasaki T., Wang, and Watanabe M. **(2003)** Redoxable nanosheet crystallites of MnO_2 derived via delamination of a layered manganese oxide. *J. Am. Chem. Soc.* 125 (12) 3568-3575.

11 Sambasivam S., Li G.J., Jeong J.H., Choi B.C., Kim S.S., and Song T.K. **(2012)** Structural, optical, and magnetic properties of single-crystalline Mn_3O_4 nanowires. *J. Nanopart. Res.* 14 (9) 1138.

12 Zhang Y.C., Qiao T., and Hu X.Y. **(2004)** Preparation of Mn_3O_4 nanocrystallites by low-temperature solvothermal treatment of γ-MnOOH nanowires. *J. Solid State Chem*. 177 (11) 4093-4097.

13 Yang L.X., Liang Y., Chen H., Meng Y.F., and Jiang W. **(2009)** Controlled synthesis of Mn_3O_4 and $MnCO_3$ in a solvothermal system. *Mater. Res. Bull*. 44 (8) 1753-1759.

14 Jensen G.B., and Nielsen O.V. **(1974)** The magnetic structure of Mn_3O_4 Hausmannite between 4.7K and Neel point, 41K. *J. Phys. C: Solid State Phys*. 7 (2) 409-424.

15 Wang N., Cao X., Lin G., and Shihe Y. **(2007)** λ-MnO_2 nanodisks and their magnetic properties. *Nanotechnology* 18 (47) 475605.